Genetic remodeling of protein glycosylation *in vivo* induces autoimmune disease

Daniel Chui*†‡, Gayathri Sellakumar*†‡, Ryan S. Green*†, Mark Sutton-Smith§, Tammie McQuistan†, Kurt W. Marek*†, Howard R. Morris§, Anne Dell§, and Jamey D. Marth*†¶

*Glycobiology Research and Training Center, Howard Hughes Medical Institute, †Department of Cellular and Molecular Medicine, University of California at San Diego, La Jolla, CA 92093; and §Department of Biochemistry, Imperial College of Science, Technology and Medicine, London SW7 2AY, England

Edited by Stuart A. Kornfeld, Washington University School of Medicine, St. Louis, MO, and approved December 1, 2000 (received for review August 9, 2000)

Autoimmune diseases are among the most prevalent of afflictions, yet the genetic factors responsible are largely undefined. Protein glycosylation in the Golgi apparatus produces structural variation at the cell surface and contributes to immune self-recognition. Altered protein glycosylation and antibodies that recognize endogenous glycans have been associated with various autoimmune syndromes, with the possibility that such abnormalities may reflect genetic defects in glycan formation. We show that mutation of a single gene, encoding α-mannosidase II, which regulates the hybrid to complex branching pattern of extracellular asparagine (N)-linked oligosaccharide chains (*N*-glycans), results in a systemic autoimmune disease similar to human systemic lupus erythematosus. α-Mannosidase II-deficient autoimmune disease is due to an incomplete overlap of two conjoined pathways in complex-type *N*-glycan production. Lymphocyte development, abundance, and activation parameters are normal; however, serum immunoglobulins are increased and kidney function progressively falters as a disorder consistent with lupus nephritis develops. Autoantibody reactivity and circulating immune complexes are induced, and anti-nuclear antibodies exhibit reactivity toward histone, Sm antigen, and DNA. These findings reveal a genetic cause of autoimmune disease provoked by a defect in the pathway of protein *N*-glycosylation.

autoimmunity | genetics | lupus | glomerulonephritis

Autoimmune diseases afflict an estimated 5% of the human population, yet inherited genetic susceptibilities and causes are for the most part unknown (1, 2). The immune system recognizes glycan-dependent features in self-/non-self-discrimination, and distinct changes in protein glycosylation have been reported in various autoimmune syndromes (3–7). The first autoantibodies to be discovered were the cold agglutinins that bind to glycan chains (termed I/i antigens) and appear to be responsible for approximately 20% of human autoimmune hemolytic anemia cases (3). Elevated levels of autoantibodies to glycolipids are noted in various neurologic disorders, including motor neuron disease (3). Altered glycosylation may also affect immune complex formation. Immunoglobulins with affinity for the Fc region of IgG molecules are found in rheumatoid arthritis, and the severity of the disease is associated with the extent of galactose-deficient *N*-glycans on Fc (8). Human IgA nephropathy has been associated with altered *O*-glycosylation of the IgA1 hinge region and Ig deposition in the kidney (9, 10). Another possible role for aberrant glycan production in autoimmune disease includes Tn syndrome, in which reduced transcription of the core 1 *O*-glycan β1–3 GalT enzyme occurs among hematopoietic compartments. This reduced transcription results in exposure of the Tn antigen on cell surfaces, and some patients suffer hemolytic anemia, thrombopenia, and leukopenia, likely because of the presence of anti-Tn antibodies found in normal serum (11).

Glycan structures can clearly participate in pathogenic processes. Yet determining whether glycan recognition and production abnormalities are a cause of autoimmune disease or are secondary events induced by lesions in other metabolic pathways has awaited studies involving *in vivo* genetic modifications of the glycosylation program itself. Golgi-resident glycosidase and glycosyltransferase enzymes operating in the glycan synthesis pathways are thereby hypothetically promising targets of genetic studies aimed at gaining further insights into the pathogenesis of autoimmune disease.

The α-mannosidase II enzyme is encoded by a single gene in mammals and resides in the Golgi apparatus, where it trims two mannose residues from hybrid N-linked oligosaccharides. This trimming of the mannose residues allows the subsequent addition of multiple glycan branches by glycosyltransferases, as required for the generation of complex *N*-glycans—the most prevalent and diverse forms found on mammalian cell surfaces (12–15). Nonerythroid cells from mice lacking a functional α-mannosidase II gene were unexpectedly found to compensate for this defect by the activity of another α-mannosidase defining an alternative pathway (Fig. 1 and ref. 14). In erythroid cells, glycoproteins were expressed normally at the cell surface, but their portfolio of attached carbohydrate structures was altered with a loss of complex *N*-glycan branching concurrent with an induction of hybrid *N*-glycan forms. These animals exhibit a non-life-threatening dyserythropoiesis similar to human congenital dyserythropoietic anemia type II (14).

We have since observed an increased morbidity of aged mice lacking α-mannosidase II and have therefore attempted to determine whether the loss of α-mannosidase II in some tissues is not fully compensated for by the alternative pathway and leads to physiologic defects among nonerythroid cell types. Our findings herein have revealed that α-mannosidase II is essential for promoting complex *N*-glycan branching to varying degrees in different tissues and cell types and on subsets of glycoproteins. The resulting alteration of *N*-glycan branching provokes a systemic autoimmune disease, indicating that inheritance of an abnormal protein *N*-glycosylation pathway is an etiologic factor in the pathogenesis of autoimmunity.

Materials and Methods

Mice. The null allele for α-mannosidase II (14) was bred into the C57BL/6 genetic background for more than eight generations before these studies. The mice were maintained in a restricted-access barrier facility under specific pathogen-free conditions.

Lectin Blotting. Membrane and total cellular proteins were isolated from various tissues, and complex *N*-glycans were visualized by binding to E-phytohemagglutinin lectin as previously described (14).

Mass Spectrometry. *N*-Glycans were isolated from protein by peptide:*N*-glycanase F (PNGase F) treatment and subjected to various

This paper was submitted directly (Track II) to the PNAS office.

Abbreviations: PFA, paraformaldehyde; PNGase F, peptide:*N*-glycanase F.

†D.C. and G.S. contributed equally to this work.

¶To whom reprint requests should be addressed at: Howard Hughes Medical Institute, 9500 Gilman Drive-0625, University of California San Diego, La Jolla, CA 92093. E-mail: jmarth@ucsd.edu.

The publication costs of this article were defrayed in part by page charge payment. This article must therefore be hereby marked "advertisement" in accordance with 18 U.S.C. §1734 solely to indicate this fact.

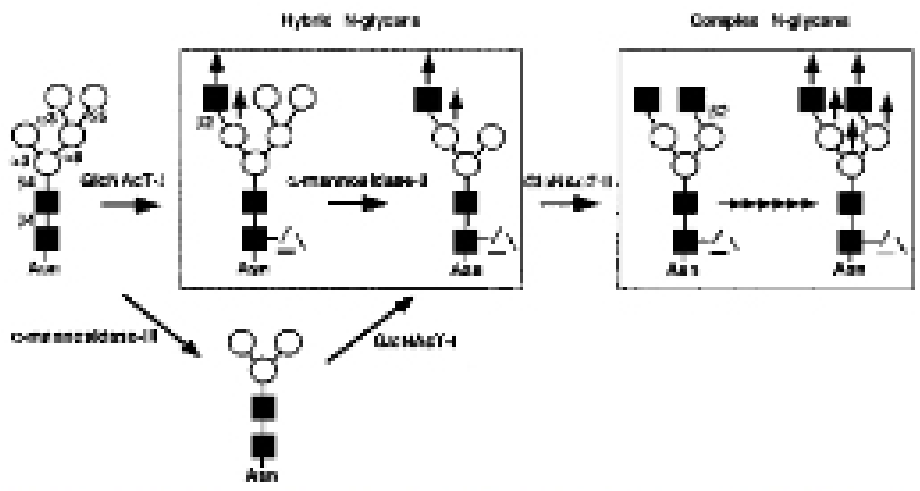

Fig. 1. Two pathways to complex protein *N*-glycosylation in mammals. Complex-type *N*-glycans are produced in the Golgi apparatus and are the predominant forms among extracellular compartments. Each pathway depends on a separate α-mannosidase activity to produce the hybrid *N*-glycan substrate for the GlcNAcT-II glycosyltransferase. Differential use of each pathway among glycoprotein substrates indicates additional controls in *N*-glycan repertoire expression. Black square, *N*-acetylglucosamine; open triangle, fucose; black circles, galactose; open circles, mannose. Anomeric linkage states are denoted. The α1–6 linkage of fucose to the asparagine-proximal *N*-acetylglucosamine (dashed lines) can be found on both hybrid and complex *N*-glycans.

glycosidases before analysis by mass spectrometry, as previously described (16).

Histology. Tissues were fixed in formalin (Fisher Scientific) for 24 h then sequentially dehydrated in increasing ethanol concentrations before they were embedded in paraffin. A microtome (Leica, Deerfield, IL) was used to obtain 3 to 5-μm paraffin sections for staining with hematoxylin and eosin. For immunofluorescence, except for anti-C3, tissues were frozen in Optimal Cutting Temperature medium (VWR Scientific) and sectioned to 3 μm. An ultramicrotome (Leica FCS) was used to obtain 1-μm sections from tissue fixed in 4% paraformaldehyde (PFA) for 1 h, followed by fixation in 8% PFA for 15 min, and cryoprotected in polyvinylpyrrolidone sucrose for analysis with anti-C3 (ICN and Cappel) at 1:50 dilution. An FITC-conjugated anti-goat secondary antibody was used to visualize anti-C3 staining. Frozen samples were fixed with acetone, rinsed with PBS, and incubated in PBS with 10% FCS for 30 min before staining with FITC-conjugated goat anti-mouse antibody specific to IgA, IgM, IgG, IgG1, IgG2a, IgG2b, or IgG3 (Southern Biotechnology Associates) at 1:500 dilution for 60 min at 22°C. Slides were washed in PBS and coverslip mounted for immunofluorescence viewing with a Zeiss Axioplan.

Electron Microscopy. Mouse kidneys were perfused with PBS (20 min) and fixed by 4% PFA for 30 min. The cortex was cut into 1-mm cubes and immersion fixed in 4% PFA (45 min) and 8% PFA (15 min). Tissues were processed, sectioned, labeled with a 10-nm gold-conjugated goat anti-mouse IgG + IgM (H + L), and examined by electron microscopy as described (17).

Urinalysis. Urine was collected from mice and tested with Multistix 10SG (Bayer, Elkhart, IN) reagent strips. Hematuria (trace–large) and proteinuria (trace–2000 mg/dl) were quantified by color. For proteinuria, a positive result was chosen as a minimum value of 100 mg/dl.

Hematology, Flow Cytometry, and Lymphoid Activation. Hematopoietic profiles of mutant mice and littermates were acquired with a CELL-DYN flow cytometer with manual differential counts on glass slides, with the use of Wright–Giemsa, as described (18). Nucleated circulating cells and single-cell suspensions of thymus, spleen, lymph nodes, and bone marrow were collected as described (18). Leukocytes were analyzed with anti-B220-FITC, CD4-FITC, IgM-phycoerythrin, Gr-1-phycoerythrin, Mac-1-FITC (PharMingen), and CD8-Tricolor (Caltag, South San Francisco, CA). Data were analyzed on a FACScan flow cytometer with CELLQUEST software (Becton Dickinson). T and B lymphocytes were purified by a negative sorting strategy following the Dynabead protocol (Dynal, Great Neck, NY). B cells were purified by the use of biotinylated anti-Thy-1.2, CD43 (S7 clone), Ter-119, NK-1.1, Gr-1, and Mac-1 (PharMingen) and streptavidin magnetic beads (Dynal). $CD4^+$ and $CD8^+$ T cells were purified by first removing B cells with Dynal sheep anti-mouse IgG magnetic beads followed by a negative sorting approach that uses biotinylated anti-Gr-1, Ter-119, NK-1.1, and one of either anti-CD4 or CD8 with streptavidin magnetic beads. Lymphoid proliferation was analyzed as described (19,20).

Serum Ig Levels. Serum Ig levels were measured as previously described (19).

Anti-nuclear Antibodies. For anti-nuclear antibody detection, mice sera were diluted to 1:250 in PBS and incubated with HEp-2 cell substrate slides (Immuno Concepts, Sacramento, CA) in a covered humidified chamber for 30 min at 22°C. Slides were rinsed in PBS for 20 min, and antibody was detected with the use of FITC-conjugated anti-mouse IgG + IgM (Jackson ImmunoResearch) at 1:250 for 30 min at 22°C. Slides were washed in PBS and mounted with coverslips for viewing. Plates coated with indicated antigens and C1q to detect circulating immune complexes (CIC) (Alpha Diagnostic International, San Antonio, TX) were used with sera diluted by 1:400 in the buffers supplied.

Autoantibody Characterization. Tissue homogenates were produced in lysis buffer (5% 1 M Tris·HCl, pH 7.5/3% 5 M NaCl/1% Triton X-100 detergent) with the use of Kontes–Duall tissue grinders (Fisher) and coated at 10 μg/ml for 1 h at 37°C into 96-well Nunc Maxisorp plates (Fisher). Plates were washed three times with 150 μl PBS with 0.05% Nonidet P-40 and incubated with 2% BSA in PBS for 1 h at 37°C. Plates were washed, and serial dilutions of wild-type and mutant sera (in PBS with 1% BSA) were added for 90 min at 37°C. Plates were washed and incubated with 100 μl of an alkaline phosphatase-conjugated anti-mouse Ig κ light-chain monoclonal antibody (PharMingen) in PBS with 1% BSA at 1:5000 for 45 min at 22°C. Plates were washed and developed with 100 μl of *p*-nitrophenyl phosphate (Sigma) for 15 min at 22°C, and reactions were stopped with 50 μl of 0.1 M EDTA. Plates were read on a VERSAmax microplate reader at 405 nm (Molecular Devices). Removal of *N*-glycans was accomplished by boiling 100 μg of homogenate for 3 min in buffer containing 50 mM sodium phosphate (pH 7.5 generated with NaH_2PO_4 and Na_2HPO_4), 0.4% SDS, and 8% 2-mercaptoethanol before the addition of 5 milliunits of PNGase F (Calbiochem) in 1% Nonidet P-40 and 2% sodium phosphate (pH 7.5). This procedure was followed by a 24-h incubation at 37°C. Tissue homogenates (20 μg) were subjected to SDS/PAGE, transferred to nitrocellulose, and incubated with 5% BSA in TBS (20 mM Tris·HCl, pH 8.0/150 mM NaCl) for 2 h. Blots were then incubated with sera (1:2000 dilution) in TBS with 1% BSA, or with biotinylated Con A (Sigma) at 50 ng/ml in TBS with 0.1 mM $MgCl_2$, 0.1 mM $MnCl_2$, 0.1 mM $CaCl_2$, 0.05% Nonidet P-40, and 1% BSA for 90 min at 22°C. Autoantibody binding was detected with the use of enhanced chemiluminescence (Amersham Pharmacia) after a 45-min incubation with a horseradish peroxidase-conjugated anti-κ light chain monoclonal antibody (PharMingen) at 1:10,000 in TBS with 0.05% Nonidet P-40. Con A binding was detected with enhanced chemiluminescence after a 45-min incubation with horseradish peroxidase-conjugated streptavidin (Vector Laboratories) at 1:10,000 in TBS with 0.05% Nonidet P-40 and an overnight wash.

Results

The degree to which the alternative α-mannosidase pathway compensates for the absence of α-mannosidase II in various

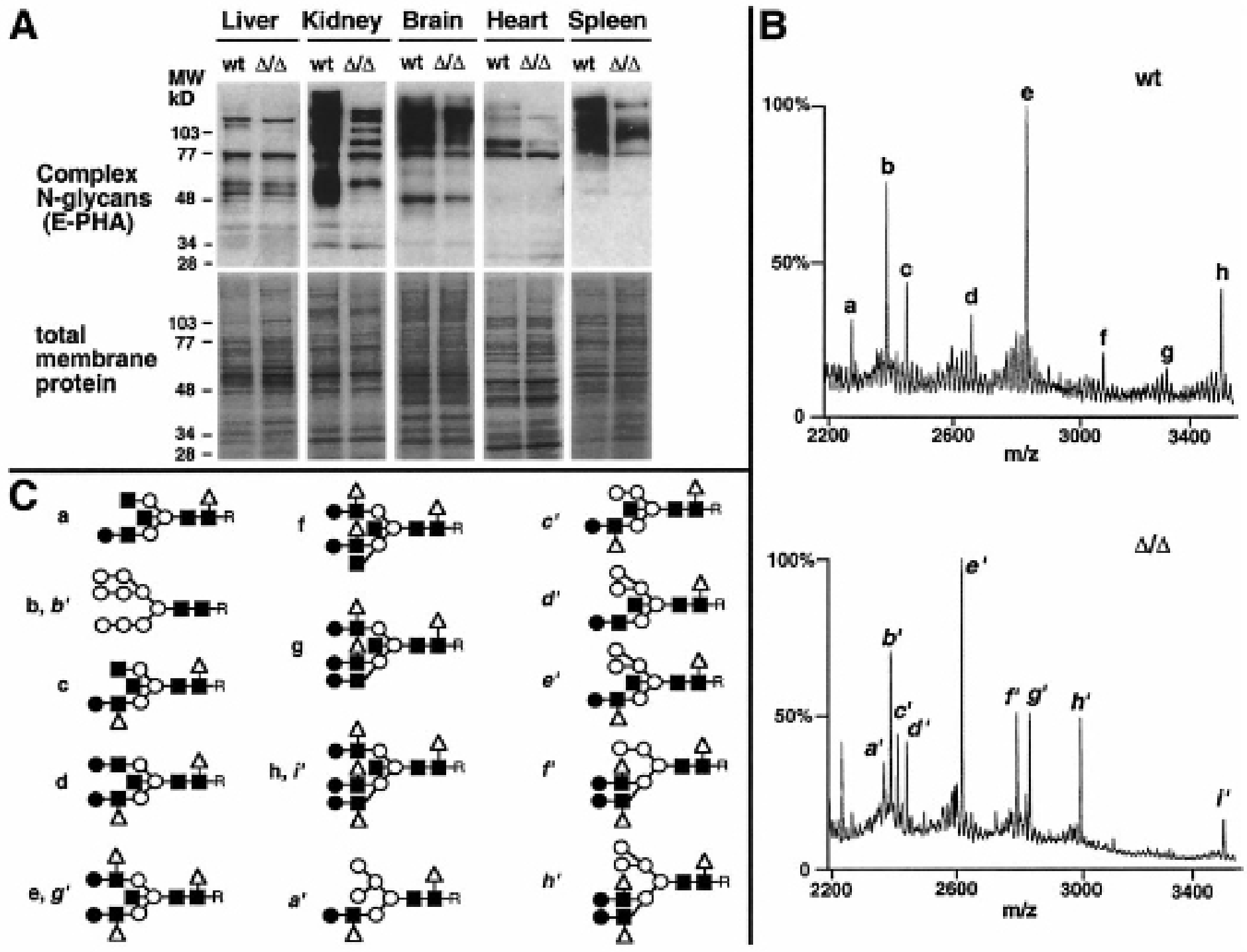

Fig. 2. Reduction in complex *N*-glycans and increased hybrid *N*-glycan structures in the absence of α-mannosidase II. (*A*) Complex *N*-glycans are deficient on glycoproteins from some tissues in mice homozygous for a deletion in the α-mannosidase II gene (Δ/Δ). Membrane protein was isolated from various tissues, and complex *N*-glycans were visualized by binding to E-phytohemagglutinin (*Upper*) as previously described (14). Equivalent amounts of membrane protein were used in the analyses (*Lower*). (*B*) Mass spectrometry of *N*-glycans from various tissues (kidney shown) was accomplished after isolation from glycoproteins by PNGase F. Subsequent treatment with various glycosidases (not shown) provided additional information on specific saccharide linkages (16). (*C*) *N*-Glycan structures (desialylated) defined by mass spectrometry from wild-type tissues were mostly complex types with fully modified mannose termini bearing *N*-acetylglucosamine linkages (*a*, *c*–*h*), whereas structures in the absence of α-mannosidase II contained hybrid *N*-glycans noted by terminal mannose residues (*a'*, *c'*, *d'*, *e'*, *f'*, *h'*). The anomeric glycosidic linkages among the core regions are indicated (Fig. 1). Antennary extensions are with β1–2-linked glucosamine, β1–4-linked galactose, and α1–6-linked fucose and are as described for the relevant Lewis antigens (38). R indicates the position of the asparagine residue before release of *N*-glycans from glycoproteins by PNGase F. For monosaccharide symbols, see Fig. 1 legend.

tissues was investigated. With the use of the E-phytohemagglutinin lectin as a probe for complex *N*-glycans, we analyzed glycoproteins derived from various organs of α-mannosidase II-deficient mice (see ***Materials and Methods***). Some glycoproteins appeared to be quantitatively affected and exhibit reduced levels of complex *N*-glycans, whereas a few appeared fully dependent on α-mannosidase II for hybrid to complex-type *N*-glycan synthesis (Fig. 2*A*). The glycosylation of kidney glycoproteins with complex *N*-glycans is especially dependent on α-mannosidase II. In contrast, various glycoproteins in different tissues did not appear to require α-mannosidase II as they retained normal E-phytohemagglutinin binding, indicating that the alternative pathway is sufficient for them to be modified appropriately with complex *N*-glycans.

With the use of recently developed mass spectrometry approaches for determining glycan structures in mammalian tissue (16), we defined the specific *N*-glycan branch structures expressed in tissues of wild-type and α-mannosidase II-deficient mice. These studies revealed a significant reduction of known complex *N*-glycans along with the induction of specific hybrid *N*-glycan structures in mice lacking α-mannosidase II (Fig. 2 *B* and *C*). Hybrid *N*-glycans are not prevalent in normal adult tissues, and two of the structures elucidated in the absence of α-mannosidase II are biantennary Lewis X hybrid *N*-glycan sequences not previously identified in any mammalian source (Fig. 2*C*, *f'* and *h'*). These data together indicate that α-mannosidase II function is varied among nonerythroid cell types by mechanisms that may involve restricted substrate access or perhaps distinct glycoprotein substrate preferences of GlcNAcT-I and α-mannosidase III. We inferred that α-mannosidase II may be uniquely essential for specific physiologic processes involving nonerythroid cells, which prompted us to closely investigate the physiology of aging α-mannosidase II-deficient mice.

A small but significant increase in mortality by 18 months of age was noted specifically among mice lacking α-mannosidase II. On histological examination of multiple organs, glomerulonephritis was detected in over 80% of more than two dozen